Heliyon 10 (2024) e34920

Contents lists available at ScienceDirect

Heliyon

journal homepage: www.cell.com/heliyon

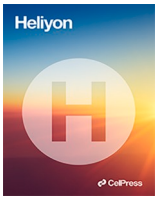

Research article

Expression and pathogenesis of insulin-like growth factor-1 and insulin-like growth factor binding protein 3 in a mouse model of ulcerative colitis

Weihua Wang [a], Xuemei Sun [b], Aina Wang [c], Yanyan Lu [a], Yue Han [a], Jianjian Zhao [a], Fuguo Liu [a,*], Zibin Tian [a,**]

[a] Department of Gastroenterology, The Affiliated Hospital of Qingdao University, Shandong, China
[b] Internal Medicine Department of Shangkou Central Health Hospital, Shandong, China
[c] Department of Gastroenterology, Shidao People's Hospital of Rongcheng, Shandong, China

ARTICLE INFO

Keywords:
Insulin-like growth factor-1
Insulin-like growth factor binding protein 3
Ulcerative colitis
Epithelial to mesenchymal transition

ABSTRACT

Background and aim: Insulin-like growth factor-1 may be involved in the epithelial-to-mesenchymal transition process. It can mitigate adverse effects when interacting with insulin-like growth factor binding protein 3. This study aimed to explore alterations in the expression of these two factors in the colonic tissue of mice with ulcerative colitis.

Method: This study utilized animal models. Mice were randomly allocated into three distinct groups. Disease activity index assessment was performed first, followed by histological grading of colitis. Protein and mRNA expression levels were determined using Western blotting and RT-qPCR. Immunohistochemical detection was used to determine histochemistry scores. Pearson correlation and SPSS 25.0 software were used for data analysis.

Results: The findings indicated a reduction in the expression of the two investigated factors as well as in epithelial-to-mesenchymal transition epithelial markers during inflammation, while the expression of noninflammatory factors increased. These effects were notably amplified following treatment. Interestingly, the changes in epithelial-to-mesenchymal transition-inducing factors and mesenchymal markers contradicted this trend. Pearson correlation analysis revealed a correlation between molecular indicators of change and epithelial-to-mesenchymal transition.

Conclusion: Insulin-like growth factor-1 and insulin-like growth factor binding protein 3 may play a protective role in the development and progression of ulcerative colitis, potentially through their inhibition of the epithelial-to-mesenchymal transition. These factors hold promise as targets for the clinical diagnosis and treatment of ulcerative colitis.

1. Introduction

Ulcerative colitis (UC) is a recurrent chronic nonspecific inflammatory bowel disease of unknown etiology that primarily affects the colonic mucosa and submucosa. Early-stage manifestations include diffuse inflammatory alterations and significant congestion in the superficial mucosa, followed by subsequent mucosal edema, erosion, and ulceration. Subsequent stages may exhibit modifications

* Corresponding author.
** Corresponding author.
E-mail addresses: liufg@qdu.edu.cn (F. Liu), tianzb@qdu.edu.cn (Z. Tian).

https://doi.org/10.1016/j.heliyon.2024.e34920
Received 21 January 2024; Received in revised form 18 July 2024; Accepted 18 July 2024
Available online 25 July 2024
2405-8440/© 2024 The Author(s). Published by Elsevier Ltd. This is an open access article under the CC BY-NC-ND license (http://creativecommons.org/licenses/by-nc-nd/4.0/).

such as intestinal wall thickening, along with shortening and narrowing of the intestinal canal [1]. Despite ongoing research, the pathogenesis of this disease remains elusive. Epithelial-to-mesenchymal transition (EMT) has emerged as pivotal in the pathophysiology of UC [2], suggesting potential targets for therapeutic intervention and prevention. EMT refers to a multistage process wherein epithelial cells undergo genetic and phenotypic changes and transform into mesenchymal cells under the influence of specific stimulating factors [3]. It is associated with various biological processes, including the inflammatory response, wound healing, tumor cell invasion, and metastasis [4,5]. The EMT process is intricately regulated by numerous cytokines and growth factors, notably epidermal growth factors, fibroblast growth factors, and vascular endothelial growth factors, among others. Alterations in the expression of these factors can activate transcription factors such as Snail, Slug, Zeb,Twist, E47, ZEB1, and ZEB2. These activations, either directly or indirectly, inhibit the expression of E-cadherin, leading to the disruption of cell tight junctions and a subsequent decrease in cytoskeleton stability [6]. EMT is orchestrated through multiple signaling pathways, notably the Wnt/β-catenin, TGF-β/Smad, PI3K/AKT, integrin, IL-6/STAT3, and NFκB pathways, among others. These pathways modulate gene expression by binding to specific cell surface receptors, consequently activating nuclear transcription factors via intracellular signal transduction [7,8]. The molecular markers primarily included cell surface markers, cytoskeletal markers, and transcription factors. E-cadherin, which is pivotal for cell-to-cell adhesion, tissue structural integrity, and cell polarity, is the foremost epithelial marker of EMT [9,10]. Additionally, there are more than 20 known varieties of cytokeratin (CK), a critical epithelial marker, with CK19 being the most extensively studied and utilized Downregulation of CK19 expression can enhance the malignant biological behavior of EMT and associated cells [11]. Cytoskeletal markers include fibroblast-specific protein 1, vimentin, and α-smooth muscle actin (α-SMA), among others. α-SMA is involved in type II epithelial–mesenchymal transition associated with tissue fibrosis [12]. The EMT-inducing factor transforming growth factor-β (TGF-β) plays a crucial role in this process. Xu et al. [13]demonstrated the ability of TGF-β1 to induce EMT via the Smad pathway. TGF-β signaling involves both Smad-dependent and Smad-independent pathways. Smad is a crucial regulatory factor in EMT and is the central mediator of EMT induced by TGF-β. Additionally, TGF-β can regulate the occurrence and progression of EMT through other signaling pathways, such as the phosphatidylinositol 3-kinase (PI3K) pathway. Yang BL et al. [14]demonstrated that the total flavonoids of Abelmoschus can inhibit the morphological changes induced by TGF-β1 in the rat intestinal epithelial cell line IEC-6. These flavonoids suppress cell migration and invasion, upregulate the expression of epithelial markers such as E-cadherin, and block the Smad signaling pathway, thereby inhibiting the epithelial–mesenchymal transition induced by TGF-β1. Inhibition of TGF-β1 increases E-cadherin expression while reducing α-SMA and *p*-Smad expression levels.

Insulin-like growth factor-1 (IGF-1) belongs to the insulin-like growth factor family, and mature IGF-1 represents the sole bioactive subunit expressed by this gene [15]. Predominantly, IGF-1 exists in its bound form, with approximately 1 % circulating in the free form within serum. Over 95 % of IGF-1 binds to insulin-like growth factor binding protein 3 (IGFBP-3) in serum [16]. This binding prevents IGF-1 from attaching to its receptors, prolongs its half-life, regulates its transport, and modulates its activity. Different concentrations of IGF-1 have varying effects on the intestinal mucosa. Optimal IGF-1 levels facilitate intestinal nutrition, mitigate epithelial cell apoptosis, and enhance proliferation [17]. Moreover, IGF-1 functions to stimulate collagen secretion, accelerating the process of wound healing [4]. However, IGF-1 overexpression induces cellular fibrosis and malignant transformation [18]. The interaction between IGF-1 and IGFBP-3 inhibits the localized release of excessive IGF-1, thereby preventing its detrimental effects. Recent research has demonstrated an association between IGF-1 and IGFBP-3 and the onset and progression of UC. In active UC patients, the expression levels of IGF-1 and IGFBP-3 are significantly lower than those in normal participants and patients in remission. Moreover, as the disease grade increases, the expression of both genes notably decreases [19,20]. These findings suggest the potential involvement of IGF-1 in UC development and its potential as a screening and treatment target. However, the precise mechanism through which IGF-1 regulates the occurrence and progression of UC remains unclear. Numerous studies have highlighted the role of IGF in the physiological process of EMT by modulating the expression of factors such as TGF-β1, P-GSK-3β, Akt, *p*-Akt, α-SMA, and others while aiding in intestinal tissue protection and injury repair [21–23]. Extensive evidence supports the notion that IGF-1 influences the biological behavior of tissues and cells by regulating EMT. Therefore, we hypothesize that IGF-1 suppresses EMT, potentially hindering the onset, progression, and prognosis of UC. The animal studies and subsequent data analysis detailed below support our hypothesis.

2. Materials and methods

2.1. Main materials

Sodium dextran sulfate (DSS) and BCA protein quantification kits were obtained from Meilun Biotechnology Co., Ltd., China. The phosphate-buffered saline (PBS), citrate buffer solution, and DAB chromogenic kit were obtained from Beijing Zhongshan Golden Bridge Biotechnology Co., Ltd. Anhydrous ethanol was obtained from Tianjin Chemical Reagent Factory. PCR and reverse transcription kits were obtained from Vazyme Biotech Co., Ltd., Nanjing. The PCR primers were supplied by Sangon Biotech Co., Ltd., Shanghai. Sterile saline solution (Model: YS-PYJ1106) was obtained from Yansheng Biotechnology Co., Ltd., Shanghai. Mesalazine enteric-coated tablets (0.25 g*36 tablets) were obtained from Tianhong Pharmaceutical Co., Ltd., with drug approval number H20103359 and batch number 20200404.

2.2. Experimental animal selection and grouping

We purchased 200 SPF male BALB/c mice (weight range: 21–24 g) aged 6–8 weeks. The mice were procured from Beijing Vitonlihua Laboratory Animal Technology Co., Ltd., and were raised at the Laboratory Animal Center of the Medical School, Qingdao University. All animal experiments were approved by the Medical Ethics Committee of the Affiliated Hospital of Qingdao University

(QYFY WZLL 28795). The mice were randomly divided into three groups: the control group (n = 60), the model group (n = 60), and the treatment group (n = 60). Each group was further divided into six subgroups. A minimum of ten mice per subgroup survived the entire experiment. This study used an animal experiment including 180 male mice. Housing conditions were maintained at 22 °C–25 °C, with 45 %–60 % relative humidity, and a 12-h light-dark cycle.

2.3. Establishment and administration of an ulcerative colitis model

A 4 % DSS solution was prepared by dissolving 400 mg of DSS in 10 ml of double-distilled water. Both the model and treatment groups received ad libitum access to drinking water containing 4 % dextran sulfate sodium (DSS) for 7 consecutive days, followed by a switch to distilled water from the 8th day onward. Conversely, the control group consumed only distilled water throughout the experiment. Beginning on the 8th day, the treatment group received mesalamine via oral gavage, which was administered at a concentration of 29.80 mg/ml twice daily at 0.2 ml per administration. The model and control groups were orally administered an equivalent volume of sterile saline. Throughout this period, all mice in each group maintained their regular dietary intake. Starting on the 8th day, both the model group and the treatment group were provided normal water and maintained in an appropriate feeding environment.

2.4. Tissue harvest and analysis

Throughout the modeling period, daily assessments included measurements of weight loss, stool consistency, and hematochezia rate in the mice. At specific time points (days 0, 4, 7, 8, 11, and 14), batches of 10 mice each were humanely euthanized using the neck-folding method. The entire colon was excised, and its length, from the ileocecal part to the anus, was recorded. The Disease Activity Index (DAI) evaluates the severity of UC. The DAI was calculated as the average score of three components. A higher total score indicates a more severe condition of UC. Subsequently, the colon was washed with precooled normal saline. A segment of the intestinal tissue was fixed in formaldehyde, embedded in paraffin, and stained with hematoxylin and eosin (HE). Evaluation of the UC histological score was conducted following the criteria outlined by Dielemen [24] et al. The assessment included more than five randomly selected high-power fields (× 400) from each region to evaluate tissue edema, ulcer length, tissue regeneration and healing, and ulcer area.

2.5. Immunohistochemical staining

We used the labeled streptavidin-biotin method to detect HE-stained sections. This method involved high-pressure antigen retrieval and subsequent inactivation of endogenous peroxidase, Anti -IGF-1, - IGFBP-3,-TGF-β1,-TGF-β1, -E-cadherin, -CK-19, and -α-SMA were used as primary antibodies and incubated at 4 °C overnight. Goat-anti-rabbit IgG was used as a secondary antibody and diaminobenzidine (DAB) staining was performed. Finally, the sections were counterstained, dehydrated, subjected to transparency treatment, and mounted. The protein expression of IGF-1, IGFBP-3, TGF-1, E-cadherin, cytokeratin, and α-SMA was examined using a light microscope. We categorized the positive grades and calculated the histochemistry score (H-score). The positive grades were determined according to predefined standards, and subsequently, the H-score was calculated. H-scores range from 0 to 300, with higher values indicating stronger and more comprehensive positive expression. Dilution Ratios of Antibodies for Immunohistochemistry in Table1.

2.6. Western blot technique

Western blotting was performed as described in a previously reported protocol [25],Protein from colon tissue was extracted using radioimmunoprecipitation assay buffer, and its concentration was determined by the standard BCA protein assay kit method. Samples containing 30 μg of protein were separated on acrylamide SDS−PAGE gels and subsequently transferred to nitrocellulose membranes. These samples were then blocked with 5 % milk and incubated overnight at 4 °C with various rabbit anti-primary antibodies: anti-IGF-1, anti-IGFBP-3, anti-E-cadherin, anti-CK-19, anti-α-SMA, anti-TGF-β1, and anti-alpha-Tubulin. After three washes with TBST for 10 min each, the membranes were exposed to a secondary antibody at room temperature for 60 min, and subsequent band detection was performed using a developer. Dilution Ratios of Antibodies for Western blot in Table2.

2.7. Real-time fluorescent quantitative polymerase chain reaction detection

The mRNA expression levels of IGF-1, IGFBP-3, TGF-β1, E-cadherin, CK-19, and α-SMA were assessed via real-time fluorescent quantitative polymerase chain reaction (qRT−PCR). Intestinal epithelial tissue was fragmented, placed in a centrifuge tube with digestive juice (0.1 % collagenase +0.1 % hyaluronic acid), and gently shaken in a 37 °C water bath for 30 min. The resulting supernatant was centrifuged at 1200 r/min for 10 min at 4 °C to isolate intestinal epithelial cells. RNA extraction was performed according to the manufacturer's instructions, and 2 μg of RNA was reverse transcribed. PCR amplification of mRNA was conducted, and the results were evaluated based on the exponential growth of the fluorescence signal, the number of quantification cycles, and the dissolution curves. RT-PCR primer sequences are listed in Table3.

2.8. Statistical analysis

In this study, the DAI score [26], colon histological score, colon length, and other indicators measured were normally distributed and are expressed as (x_± s). Statistical analysis was performed by IBM SPSS version 26.0. All variables were expressed in mean ± SD format. For group comparisons, the F test was used, while for pairwise comparisons, the LSD test was used. The significance level was set at $\alpha = 0.05$. Difference was considered significant when $p < 0.05$.

Additionally, ImageJ software was used for optical density analysis to assess the protein content. Pearson correlation analysis was used to examine the relationship between the immunohistochemical detection results (H value) of the IGF-1 and IGFBP-3 proteins and those of EMT-related marker proteins in the colon tissues of mice within the model and treatment groups.

3. Results

Comparison of DAI scores, colon histological scores and colon lengths among the three groups of experimental animals.

Before modeling (0 d), no significant differences were observed in the DAI, colon histological score, or colon length among the three groups ($P > 0.05$). However, on the 11th and 14th days, the DAI score in the treatment group was significantly lower than that in the model group ($P < 0.05$), accompanied by a longer colon length in the treatment group than in the model group ($P < 0.05$) but a shorter colon length in the treatment group than in the control group ($P < 0.05$). Furthermore, the histological score of the colon in the treatment group was notably lower than that in the model group on the 8th, 11th, and 14th days ($P < 0.05$). In the model group, the histological and DAI scores significantly increased from day 0 to day 14, while the colon length decreased, and these differences were statistically significant among the groups ($P < 0.05$). Conversely, in the treatment group, the histological and DAI scores initially increased and then gradually decreased after the 8th day. Similarly, the colon length initially decreased and gradually recovered after the 8th day, with statistically significant differences among the groups ($P < 0.05$) (Figs. 1–3).

Comparisons among the three groups of experimental animals for protein and mRNA expression levels of IGF-1, IGFBP-3, TGF-β1, E-cadherin, CK-19, and α-SMA in colon tissues.

Before modeling (0 d), there were no significant differences in the protein or mRNA expression levels of IGF-1, TGF-β1, IGFBP-3, E-cadherin, CK-19, or α-SMA among the three groups of colonic tissues ($P > 0.05$). Posttreatment, the IGF-1, CK-19, IGFBP-3, and E-cadherin expression levels in the treatment group gradually increased compared to those in the model group. TGFβ1 protein expression was lower in the treatment group than in the control group on the 11th and 14th days ($P < 0.05$), and the α-SMA protein level remained consistently lower in the treatment group ($P < 0.05$). Within-group observations revealed initial decreases followed by increases in IGF-1, E-cadherin, and CK-19 protein expression postintervention in the treatment group, while TGF-β1 and α-SMA protein expression initially increased and later decreased after treatment, with statistical significance ($P < 0.05$). Compared with those in the model group, the mRNA expression levels of TGF-β1, E-cadherin, CK-19, IGFBP-3, and IGF-1 in the treatment group increased progressively, whereas α-SMA mRNA expression was lower in the model group ($P < 0.05$). Intragroup analysis revealed initial decreases followed by increases in IGF-1, E-cadherin, and CK-19 mRNA expression posttreatment, while TGF-β1 decreased posttreatment. Conversely, the α-SMA mRNA level initially increased and then decreased after treatment, and these differences were statistically significant ($P < 0.05$) (Fig. 4).

Correlation between the H values of IGF-1 and IGFBP-3 proteins and those of EMT-related molecules in the colon tissue of mice from both the model and treatment groups.

A Pearson correlation analysis of the relationships between immunohistochemical detection of the IGF-1 and IGFBP-3 proteins (H value) and the TGF-β1, α-SMA, E-cadherin, and CK19 proteins (H value) in the colon tissues of mice from the model and treatment groups was performed. IGF-1 and IGFBP-3 exhibited negative correlations with TGF-β1 and α-SMA ($P < 0.05$) and positive correlations

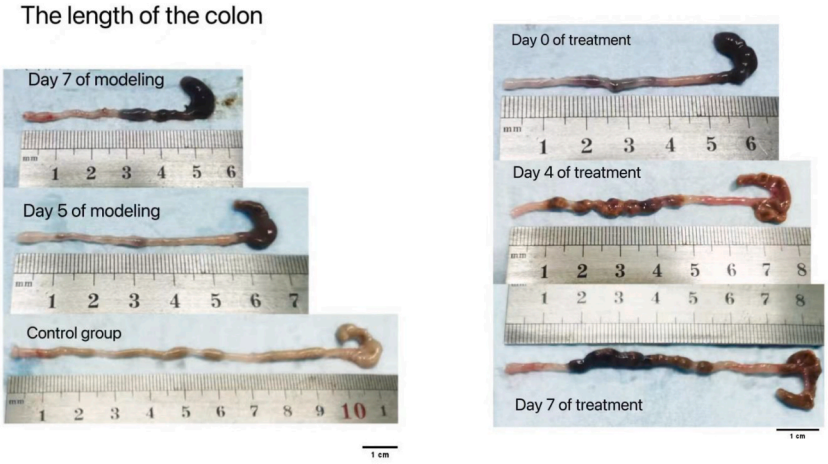

Fig. 1. Examples of partial colonic length measurements.

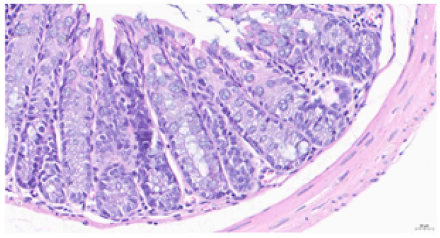

1A

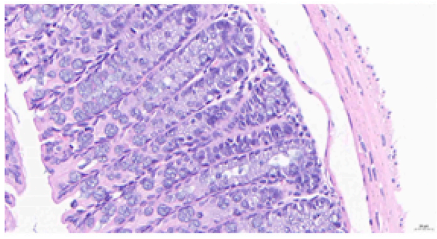

1B

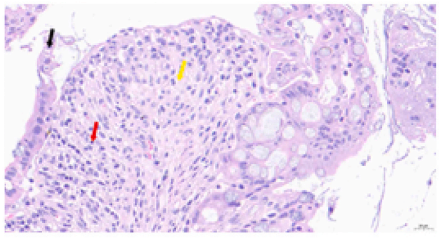

2A

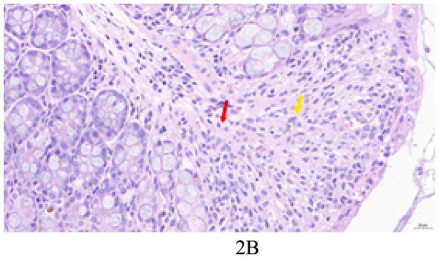

2B

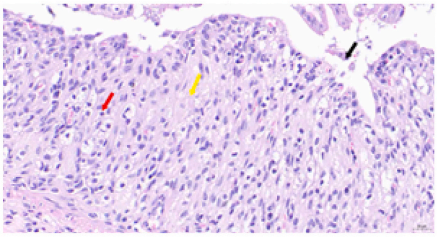

3A

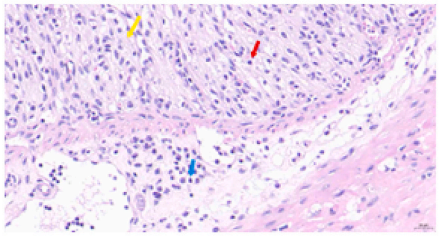

3B

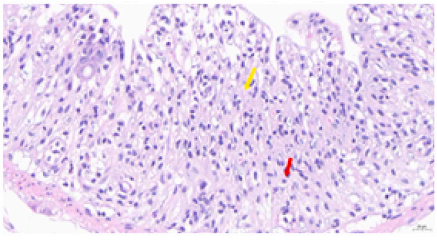

4A

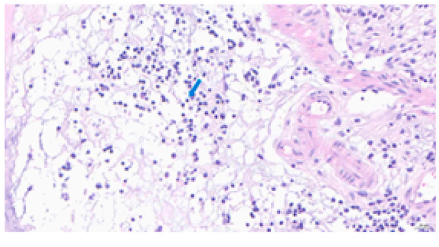

4B

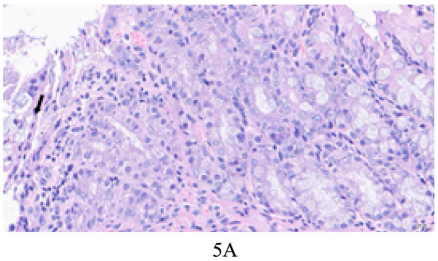

5A

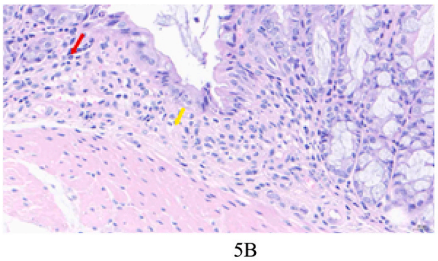

5B

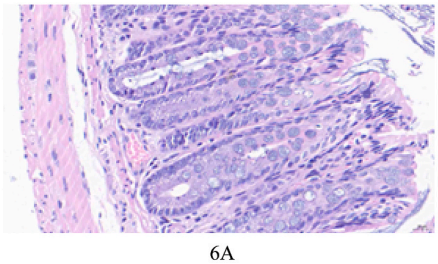

6A

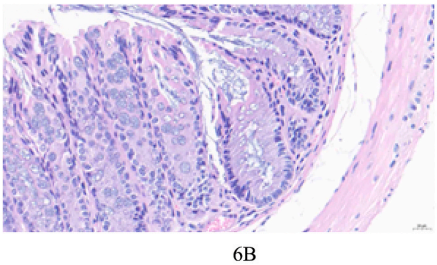

6B

(caption on next page)

Fig. 2. Illustration of the varying pathological manifestations of the mouse colon at different stages (× 40).
Note: Fig. 1A–B, 2A-2B, 3A-3B, 4A-4B, 5A-5B, and 6A-6B illustrate the pathological manifestations of the colon at different time points: d0, d4, d7, d8, d11, and d14, respectively. The following specific indicators are highlighted: a black arrow denotes necrosis and exfoliation of mucosal epithelial cells in the mucosa layer, a yellow arrow represents necrosis and disappearance of intestinal glands in the lamina propria, a red arrow indicates inflammatory cell infiltration in the lamina propria, and a blue arrow marks inflammatory cell infiltration in the submucosa.

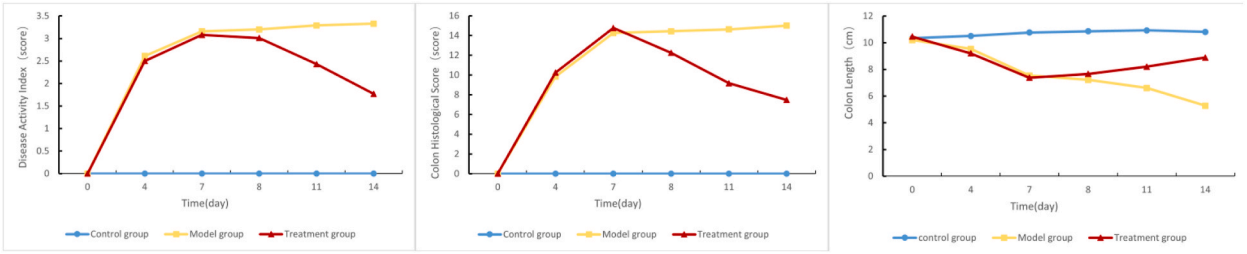

Fig. 3. Trend chart illustrating changes in the intestinal disease activity index, histological score, and colon length in mice.
Note:Control group:n = 10 control, Model group:n = 10, Treatment group:n = 10.

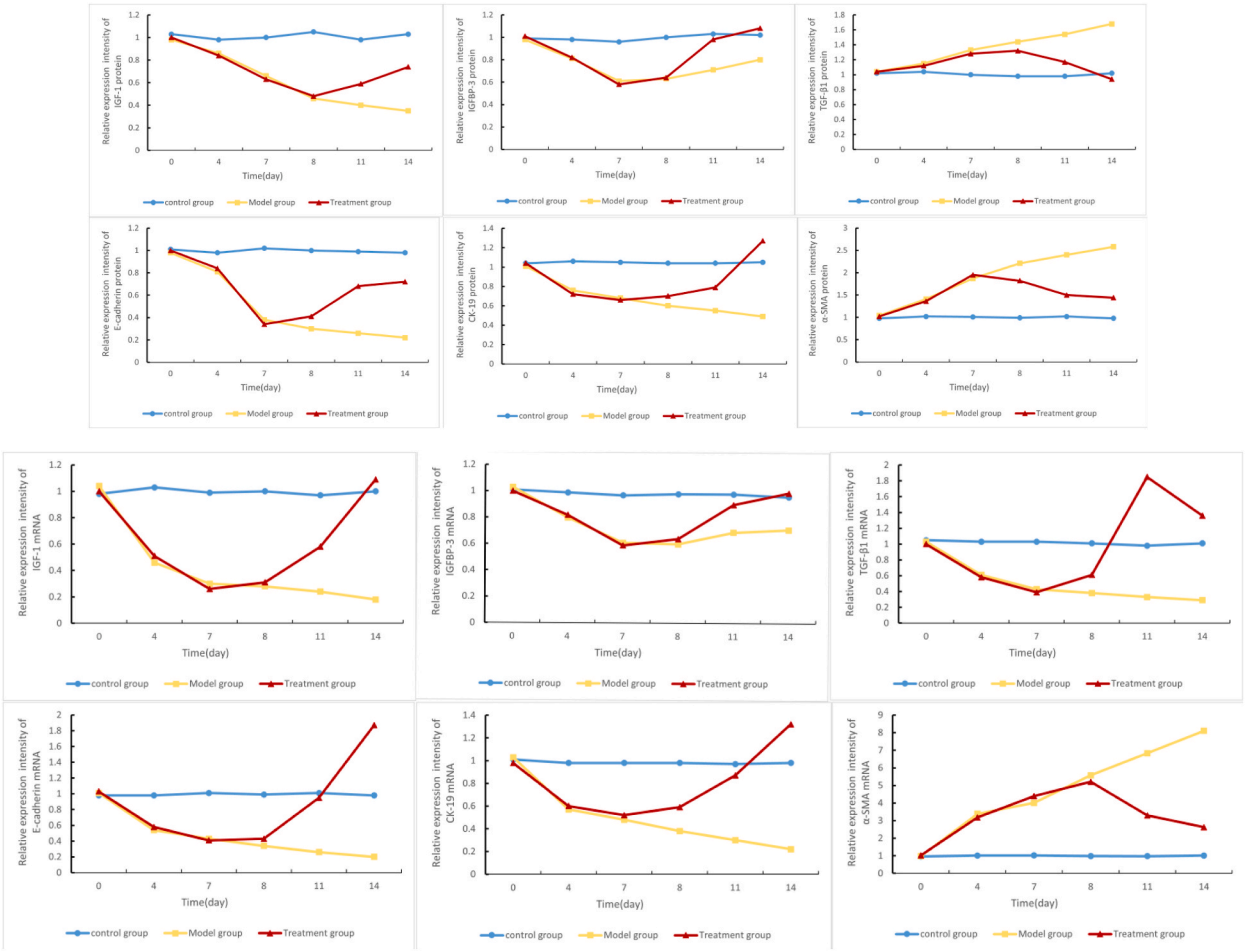

Fig. 4. Changes in the protein and mRNA expression levels of IGF-1, IGFBP-3, and EMT-related molecules in the colonic tissue of the three groups of experimental animals.
The Changing trend of protein expression levels related molecules
Note:Control group:n = 10 control, Model group:n = 10, Treatment group:n = 10
The Changing trend of mRNA expression levels related molecules
Note:Control group:n = 10 control, Model group:n = 10, Treatment group:n = 10.

with E-cadherin and CK19 ($P < 0.05$), with statistically significant correlation coefficients ($P < 0.05$). Specifically, on the 14th day, the H value of the IGF-1 protein was negatively correlated with the TGF-β1 and α-SMA expression levels and was significantly positively correlated with the E-cadherin expression level ($P < 0.05$). While a positive correlation with CK19 was observed, the correlation coefficient lacked significance ($P > 0.05$). On the 14th day, the H value of the IGFBP-3 protein in mouse colon tissue was negatively correlated with that of TGF-β1 and α-SMA and positively correlated with that of E-cadherin and CK19. Notably, the correlation between IGFBP-3 and α-SMA protein levels was statistically significant ($P < 0.05$), while the other correlations were not significant ($P > 0.05$). Detailed correlation analysis results are depicted in Table 1, and scatterplots are illustrated in Fig. 5.

Table 4: Correlations between the expression of IGF-1, IGFBP-3, and EMT-related molecules in the model group and treatment group on d7 and d14 (H value)

Note: On day 7, Figures A to D represent scatter plots demonstrating the correlation sequence between TGF-β1, α-SMA, E-cadherin,

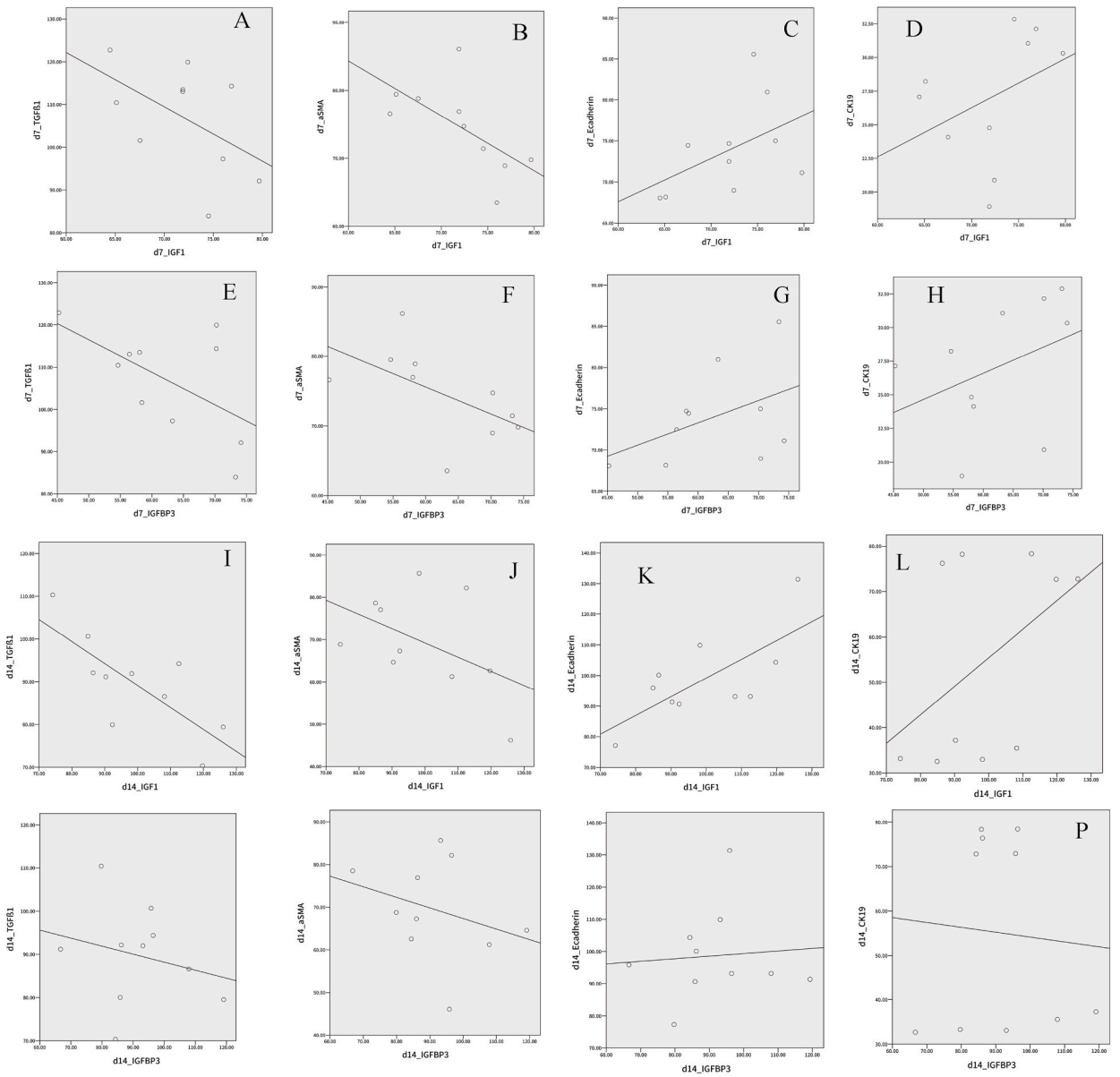

Fig. 5. Scatter plot of the correlation between IGF-1, IGFBP-3, and the expression of EMT-related molecules in the model group and treatment group on days 7 and 14

Note: On day 7, Figures A to D represent scatter plots demonstrating the correlation sequence between TGF-β1, α-SMA, E-cadherin, CK19, and IGF-1, while Figures E to H depict the correlation sequence between TGF-β1, α-SMA, E-cadherin, CK19, and IGFBP-3. On day 14, fig. I to L show the correlations between TGF-β1, α-SMA, E-cadherin, CK19, and IGF-1, and Figures M to P show the correlations between TGF-β1, α-SMA, E-cadherin, CK19, and IGFBP-3.

CK19, and IGF-1, while Figures E to H depict the correlation sequence between TGF-β1, α-SMA, E-cadherin, CK19, and IGFBP-3. On day 14, Fig. I to L show the correlations between TGF-β1, α-SMA, E-cadherin, CK19, and IGF-1, and Figures M to P show the correlations between TGF-β1, α-SMA, E-cadherin, CK19, and IGFBP-3.

4. Discussion

In the later stages of UC, thickening of the intestinal wall, narrowing and shortening of the intestinal canal, and the emergence of fibrotic lesions are observed [27,28]. There is no consensus on the causative factors behind UC. Factors contributing to its pathogenesis include infections, heredity, immunity, diet, environment, and mental and psychological aspects, among others. Notably, abnormal immune responses and regulation significantly influence this condition [29].In recent years, extensive research into the cytokine pathway has revealed the pivotal involvement of the growth hormone (GH)-suppressor of cytokine signaling protein 2 (SOCS2)- IGF-1 axis in intestinal mucosal barrier injury and repair processes. This axis, comprising GH, SOCS2, and IGF-1, promotes the differentiation and proliferation of intestinal epithelial cells. Specifically, IGF-1 contributes to cell proliferation, differentiation, and antiapoptotic resistance in intestinal epithelial cells [30–33]. Within the IGFBP family, IGFBP-3, a secreted protein found in blood and tissues, exhibits the highest affinity for IGF-1. Its primary role involves regulating IGF-1 bioactivity, facilitating the proliferation, differentiation, and apoptosis of intestinal epithelial cells, and contributing to the repair of the intestinal mucosal barrier. Previous studies have indicated that GH and IGF-1 stimulate myoid fibroblasts beneath the lamina propria epithelium, encouraging collagen secretion to aid in lesion healing. However, excessive GH or IGF-1 expression can lead to an overgrowth of intestinal muscles and interstitial cells, along with excessive collagen deposition, resulting in intestinal tumors and fibrosis. Consequently, this leads to thickening and narrowing of the intestinal wall, resulting in shortened intestinal canals. Lowering GH/IGF-1 expression to a normal level may mitigate damage to the in UC patients [34–36]. IGFs, polypeptides structurally akin to insulin, compete for insulin receptor binding sites, generating insulin-like effects. IGF-1, present in various body tissues, mainly exerts its biological function by binding to the IGF-1 receptor (IGF-1R) on cell surfaces [37,38]. IGF-1 binds to the alpha subunit of IGF-1R, phosphorylating tyrosine kinase (TK). This activation propagates downstream signaling through the PI3K-AKT1-mTOR and MAPK pathways. IGF-1R also binds to SHC, which interacts with growth factor receptor-bound protein 2 (GRB2) and son of sevenless (SOS), thereby activating the MAPK pathway [39]. In addition, downstream gene expression can be regulated by the ERK and JAK/STAT pathways. The gastrointestinal tract is a significant target of IGF-1 [40–43].

Recent research has highlighted the pivotal role of the EMT in UC pathogenesis, which is marked by three distinct alterations. Initially, EMT induces notable changes in epithelial cell morphology, resulting in the loss of polarity, a spindle-shaped appearance, and widened intercellular gaps. These shifts signify reduced cell adhesion, facilitating pseudopodia extension and enhanced mobility. Second, EMT decreases the expression of epithelial markers such as E-cadherin and catenin. Third, it prompts cells to acquire interstitial characteristics, manifested by heightened expression of interstitial markers such as N-cadherin and vimentin [44,45]. Additionally, in certain instances, it can stimulate the production of ECM hydrolases, fostering cell migration and invasion and facilitating cellular movement beyond the basement membrane into interstitial or distant tissues [5,46,47]. In this study, mice received 4 % DSS freely to establish a UC model. The results indicated a significant decrease in both body weight and colon length in the model and treatment groups between days 4 and 7 post-experiment. The disease activity index gradually increased within the first 7 days. On days 4 and 7, colon tissues displayed typical UC-associated pathological changes in both the model and treatment groups, confirming successful model establishment. EMT-inducing molecules and markers were assessed using qRT−PCR and Western blot experiments. The findings revealed a substantial increase in TGF-β1 expression during UC model induction (day 1 to day 7), peaking on day 7. Following DSS withdrawal and cessation of Mesalazine intervention, the expression levels of these genes decreased, and the pathological manifestations of the colonic mucosa were mitigated. CK19 and E-cadherin expression notably decreased during UC model induction, peaking at day 7/day 8 and rebounding after DSS discontinuation and cessation of Mesalazine intervention. Later in the treatment phase, the treatment group exhibited higher protein levels of E-cadherin and CK19 than did the control group. Conversely, the expression of α-SMA exhibited an opposite trend to that of CK19 and E-cadherin, gradually increasing during modeling and significantly decreasing after DSS cessation and the commencement of drug treatment. These findings suggest a significant role for EMT in the onset, progression, and outcomes of UC. This study reaffirmed the pivotal involvement of EMT in UC development and confirmed the protective influence of IGF-1/IGFBP-3. However, the precise mechanism by which IGF-1 affects UC progression and outcomes remains unclear. Based on our findings, IGF-1 potentially inhibits EMT, lessens colonic mucosa damage and aids in tissue repair. Correlation analysis revealed a negative correlation between the expression levels of IGF-1, IGFBP-3, TGF-β1 (EMT inducer), and α-SMA (interstitial marker) but a positive correlation between CK19 and E-cadherin (epithelial marker) in the colon tissue of both the model and treatment group mice on day 7. Nonetheless, this correlation appeared to diminish by day 14, likely due to factors regressing to physiological levels post-DSS discontinuation and treatment intervention (Mesalazine). Based on these findings, IGF-1/IGFBP-3 exhibit the potential to modulate EMT, thereby impeding UC progression, mitigating colonic tissue injury, slowing tissue fibrosis, and fostering the postinjury healing processes. EMT inhibition may help control the progression of UC. Restoration of the expression of IGF-1 and IGFBP-3 in intestinal tissue through self-repair mechanisms or exogenous interventions may inhibit EMT, reduce inflammatory injury, and promote the recovery of intestinal structure and function. The significance of IGF-1 and IGFBP-3 expression in the clinical diagnosis and treatment of UC has been confirmed by several studies. For example, intravenous infusion of T-mesenchymal stem cells can increase circulating IGF-1 levels, alleviating colitis symptoms in mice [48]. Additionally, recombinant *Lactococcus lactis* and IGF-1 secreted by ghrelin have shown significant therapeutic effects in mouse models of enteritis [49,50].

However, in tumor-related research, the effect of IGF-1 on EMT is the opposite. For example, studies on brain cancer have shown that inhibition of the PI3K/Akt signaling pathway can suppress IGF-1-mediated EMT, thereby inhibiting the malignant behavior of

brain cancer cells [51]. This may be due to the overexpression of IGF-1 in malignant tumors and other diseases, which promotes EMT and enhances the invasion and migration of tumor cells. In contrast, appropriate levels of IGF-1 and IGFBP-3 in UC intestinal tissue can inhibit EMT, promote injury repair, and alleviate UC-related pathological manifestations.

In this study, IGF-1 is presumed to inhibit EMT during UC progression, yet the precise underlying mechanisms and signaling pathways remain elusive, necessitating further research. This study investigated the molecular involved, aiming to underpin the future application of IGF-1 in clinical diagnosis, treatment, and UC prevention. However, the study was confined to histological scrutiny, lacking exploration into the specific mechanisms of IGF-1 and IGFBP-3, as well as the upstream and downstream regulatory mechanisms involved. We anticipate that future cytological and molecular biological research will allow us to better understand its regulatory mechanism and related signaling pathways. This will provide the basis for its clinical application. It is also possible that IGF-1 and IGFBP-3 exert protective effects by regulating numerous biological processes, such as EMT. In conclusion, IGF-1 and IGFBP-3 may play a protective role in the occurrence and progression of UC, reduce damage to the colonic mucosa and promote the repair of damage, and the specific mechanism may be related to the inhibition of EMT. IGF-1 and IGFBP-3 are promising targets for the clinical diagnosis and treatment of UC.

Data availability statement

The datasets used and/or analyzed during the current study are available from the corresponding author or first author upon reasonable request.

Ethics declarations

This study was reviewed and approved by the Medical Ethics Committee of the Affiliated Hospital of Qingdao University, with the approval number: QYFY WZLL 28795.

Funding

This study was supported by the Affiliated Hospital of Qingdao University Youth Research.funded projects (project no. 2828).

Disclosure of potential conflicts of interest

None.

Additional information

No additional information is available for this paper.

CRediT authorship contribution statement

Weihua Wang: Writing – original draft, Visualization, Methodology, Investigation. **Xuemei Sun:** Writing – original draft, Software, Methodology. **Aina Wang:** Resources, Project administration, Formal analysis, Data curation. **Yanyan Lu:** Validation, Supervision, Software, Resources. **Yue Han:** Validation, Supervision, Software, Project administration. **Jianjian Zhao:** Visualization, Investigation, Formal analysis, Data curation. **Fuguo Liu:** Writing – review & editing, Visualization, Investigation, Funding acquisition. **Zibin Tian:** Writing – review & editing, Project administration, Formal analysis, Data curation.

Declaration of competing interest

The authors declare that they have no known competing financial interests or personal relationships that could have appeared to influence the work reported in this paper.

Acknowledgement statement

I would like to thank all the authors for our joint efforts, the financial support from the Affiliated Hospital of Qingdao University Youth Research, and the language editing services provided by AJE.

Appendix A. Supplementary data

Supplementary data to this article can be found online at https://doi.org/10.1016/j.heliyon.2024.e34920.

References

[1] T.C. Liu, T.S. Stappenbeck, Genetics and pathogenesis of inflammatory bowel disease, Annu. Rev. Pathol. 11 (2016) 127–148.
[2] M. Guz, et al., Elevated miRNA inversely correlates with E-cadherin gene expression in tissue biopsies from crohn disease patients in contrast to ulcerative colitis patients, BioMed Res. Int. 2020 (2020) 4250329.
[3] D.C. Macias-Ceja, et al., Role of the epithelial barrier in intestinal fibrosis associated with inflammatory bowel disease: relevance of the epithelial-to mesenchymal transition, Front. Cell Dev. Biol. 11 (2023) 1258843.
[4] J. Cosnes, et al., Epidemiology and natural history of inflammatory bowel diseases, Gastroenterology 140 (6) (2011) 1785–1794.
[5] D.M. Gonzalez, D. Medici, Signaling mechanisms of the epithelial-mesenchymal transition, Sci. Signal. 7 (344) (2014) re8.
[6] M. Scharl, et al., Potential role for SNAIL family transcription factors in the etiology of Crohn's disease-associated fistulae, Inflamm. Bowel Dis. 17 (9) (2011) 1907–1916.
[7] A. Dongre, R.A. Weinberg, New insights into the mechanisms of epithelial-mesenchymal transition and implications for cancer, Nat. Rev. Mol. Cell Biol. 20 (2) (2019) 69–84.
[8] N. Zidar, et al., Down-regulation of microRNAs of the miR-200 family and up-regulation of Snail and Slug in inflammatory bowel diseases - hallmark of epithelial-mesenchymal transition, J. Cell Mol. Med. 20 (10) (2016) 1813–1820.
[9] H. Lu, et al., Reflux conditions induce E-cadherin cleavage and EMT via APE1 redox function in oesophageal adenocarcinoma, Gut 73 (1) (2023) 47–62.
[10] T.Y. Na, et al., The functional activity of E-cadherin controls tumor cell metastasis at multiple steps, Proc Natl Acad Sci U S A 117 (11) (2020) 5931–5937.
[11] N.A. Kuburich, et al., Vimentin and cytokeratin: good alone, bad together, Semin. Cancer Biol. 86 (Pt 3) (2022) 816–826.
[12] R. Sferra, et al., Interaction between sphingosine kinase/sphingosine 1 phosphate and transforming growth factor-β/Smads pathways in experimental intestinal fibrosis. An in vivo immunohistochemical study, Eur. J. Histochem. 62 (3) (2018).
[13] S. Xu, et al., Curcumin suppresses intestinal fibrosis by inhibition of PPARgamma-mediated epithelial-mesenchymal transition, Evid Based Complement Alternat Med 2017 (2017) 7876064.
[14] B.L. Yang, et al., Total flavone of Abelmoschus manihot suppresses epithelial-mesenchymal transition via interfering transforming growth factor-beta1 signaling in Crohn's disease intestinal fibrosis, World J. Gastroenterol. 24 (30) (2018) 3414–3425.
[15] A. Kasprzak, W. Szaflarski, Role of alternatively spliced messenger RNA (mRNA) isoforms of the insulin-like growth factor 1 (IGF1) in selected human tumors, Int. J. Mol. Sci. 21 (19) (2020).
[16] A.I. Martin, et al., IGF-1 and IGFBP-3 in inflammatory cachexia, Int. J. Mol. Sci. 22 (17) (2021).
[17] S.J. Geffken, et al., Insulin and IGF-1 elicit robust transcriptional regulation to modulate autophagy in astrocytes, Mol Metab 66 (2022) 101647.
[18] Z. Zhang, et al., The effects of different doses of IGF-1 on cartilage and subchondral bone during the repair of full-thickness articular cartilage defects in rabbits, Osteoarthritis Cartilage 25 (2) (2017) 309–320.
[19] M. Krakowska-Stasiak, et al., Insulin-like growth factor system in remission and flare of inflammatory bowel diseases, Pol. Arch. Intern. Med. 127 (12) (2017) 832–839.
[20] S.C. Kim, P.H. Hwang, Up-regulation of IGF binding protein-3 inhibits colonic inflammatory response, J Korean Med Sci 33 (13) (2018) e110.
[21] A. Cevenini, et al., Molecular signatures of the insulin-like growth factor 1-mediated epithelial-mesenchymal transition in breast, lung and gastric cancers, Int. J. Mol. Sci. 19 (8) (2018).
[22] L. Chen, et al., Vitamin D3 induces mesenchymal-to-endothelial transition and promotes a proangiogenic niche through IGF-1 signaling, iScience 24 (4) (2021) 102272.
[23] Z.F. Yin, et al., Buyang Huanwu Tang inhibits cellular epithelial-to-mesenchymal transition by inhibiting TGF-beta1 activation of PI3K/Akt signaling pathway in pulmonary fibrosis model in vitro, BMC Complement Med Ther 20 (1) (2020) 13.
[24] L.A. Dieleman, et al., Chronic experimental colitis induced by dextran sulphate sodium (DSS) is characterized by Th1 and Th2 cytokines, Clin. Exp. Immunol. 114 (3) (1998) 385–391.
[25] S.C. Taylor, et al., A defined methodology for reliable quantification of Western blot data, Mol. Biotechnol. 55 (3) (2013) 217–226.
[26] S. Wirtz, et al., Chemically induced mouse models of acute and chronic intestinal inflammation, Nat. Protoc. 12 (7) (2017) 1295–1309.
[27] Y. Liu, et al., Camellia sinensis and litsea coreana ameliorate intestinal inflammation and modulate gut microbiota in dextran sulfate sodium-induced colitis mice, Mol. Nutr. Food Res. 64 (6) (2020) e1900943.
[28] I. Ordas, et al., Ulcerative colitis, Lancet 380 (9853) (2012) 1606–1619.
[29] T. Zuo, et al., Gut mucosal virome alterations in ulcerative colitis, Gut 68 (7) (2019) 1169–1179.
[30] C. Farquharson, S.F. Ahmed, Inflammation and linear bone growth: the inhibitory role of SOCS2 on GH/IGF-1 signaling, Pediatr. Nephrol. 28 (4) (2013) 547–556.
[31] R. Dobie, et al., Suppressor of cytokine signaling 2 (Socs2) deletion protects bone health of mice with DSS-induced inflammatory bowel disease, Dis Model Mech 11 (1) (2018).
[32] A. Al-Araimi, et al., Deletion of SOCS2 reduces post-colitis fibrosis via alteration of the TGFbeta pathway, Int. J. Mol. Sci. 21 (9) (2020).
[33] C. Soendergaard, et al., Characterization of growth hormone resistance in experimental and ulcerative colitis, Int. J. Mol. Sci. 18 (10) (2017).
[34] B.W. Warner, The pathogenesis of resection-associated intestinal adaptation, Cell Mol Gastroenterol Hepatol 2 (4) (2016) 429–438.
[35] S.W. Longshore, et al., Bowel resection induced intestinal adaptation: progress from bench to bedside, Minerva Pediatr. 61 (3) (2009) 239–251.
[36] K. Chen, et al., Insulin-like growth factor-1 modulation of intestinal epithelial cell restitution, JPEN J Parenter Enteral Nutr 23 (5 Suppl) (1999) S89–S92.
[37] H. Yao, et al., Fully automated endoscopic disease activity assessment in ulcerative colitis, Gastrointest. Endosc. 93 (3) (2021) 728–736 e1.
[38] T. Yoshida, P. Delafontaine, Mechanisms of IGF-1-mediated regulation of skeletal muscle hypertrophy and atrophy, Cells 9 (9) (2020).
[39] T.R. Graham, et al., Insulin-like growth factor-I-dependent up-regulation of ZEB1 drives epithelial-to-mesenchymal transition in human prostate cancer cells, Cancer Res. 68 (7) (2008) 2479–2488.
[40] W.T. Iams, C.M. Lovly, Molecular pathways: clinical applications and future direction of insulin-like growth factor-1 receptor pathway blockade, Clin. Cancer Res. 21 (19) (2015) 4270–4277.
[41] E. Himpe, R. Kooijman, Insulin-like growth factor-I receptor signal transduction and the Janus Kinase/Signal Transducer and Activator of Transcription (JAK-STAT) pathway, Biofactors 35 (1) (2009) 76–81.
[42] H. Zatorski, M. Marynowski, J. Fichna, Is insulin-like growth factor 1 (IGF-1) system an attractive target inflammatory bowel diseases? Benefits and limitation of potential therapy, Pharmacol. Rep. 68 (4) (2016) 809–815.
[43] V. Lorenzo-Zúñiga, et al., Insulin-like growth factor I improves intestinal barrier function in cirrhotic rats, Gut 55 (9) (2006) 1306–1312.
[44] S.J. Serrano-Gomez, M. Maziveyi, S.K. Alahari, Regulation of epithelial-mesenchymal transition through epigenetic and post-translational modifications, Mol. Cancer 15 (2016) 18.
[45] M. Sommariva, N. Gagliano, E-Cadherin in pancreatic ductal adenocarcinoma: a multifaceted actor during EMT, Cells 9 (4) (2020).
[46] H. Tian, et al., Biophysics role and biomimetic culture systems of ECM stiffness in cancer EMT, Glob Chall 6 (6) (2022) 2100094.
[47] G.D. Marconi, et al., Epithelial-mesenchymal transition (EMT): the type-2 EMT in wound healing, tissue regeneration and organ fibrosis, Cells 10 (7) (2021).
[48] J. Xu, et al., Embryonic stem cell-derived mesenchymal stem cells promote colon epithelial integrity and regeneration by elevating circulating IGF-1 in colitis mice, Theranostics 10 (26) (2020) 12204–12222.

[49] P. Ceranowicz, et al., Essential role of growth hormone and IGF-1 in therapeutic effect of ghrelin in the course of acetic acid-induced colitis, Int. J. Mol. Sci. 18 (6) (2017).
[50] S. Liu, et al., Recombinant Lactococcus lactis expressing porcine insulin-like growth factor I ameliorates DSS-induced colitis in mice, BMC Biotechnol. 16 (2016) 25.
[51] Y.C. Lin, et al., Osthole inhibits insulin-like growth factor-1-induced epithelial to mesenchymal transition via the inhibition of PI3K/Akt signaling pathway in human brain cancer cells, J. Agric. Food Chem. 62 (22) (2014) 5061–5071.